MAGNETIC FIELD ENHANCEMENT OF THE QUAD CONFINEMENT THRUSTER (QCT): DESIGN AND EARLY DEVELOPMENT OF THE QCT PHOENIX

SPACE PROPULSION 2020
ESTORIL, PORTUGAL / 17 – 19 MARCH 2021

E. Rosati Azevedo [(1)], V.G. Tirila [(1)], A. Schwertheim [(1)], A. Knoll [(1)]

[(1)] *Imperial College London, London (United Kingdom), Email:*
emmanuelle.azevedo13@alumni.imperial.ac.uk

KEYWORDS: electric propulsion, plasma propulsion, electromagnetic modelling, thrust vectoring.

ABSTRACT:
The Quad Confinement Thruster (QCT) is a promising novel electromagnetic device designed for low power Electric Propulsion (EP) [1, 2]. While the QCT presents certain advantages over alternative commercially available technologies, such as the ability to vector thrust, it has showcased poor thrust efficiency. Ion velocity measurements taken in the thruster's plume revealed this was due to the shape of the ion acceleration front and further pointed to a potential link between the location of the acceleration front and the electromagnetic topology of the thruster [3]. The authors built a 3D model of the thruster's magnetic field to investigate the nature of this link. Analysis of the model gave sufficient insight to allow the conceptual design of a new version of the thruster, the QCT Phoenix. Subsequent detailed mechanical design of the QCT Phoenix is guided by thermal and cost related constraints. Thermal failure modes are identified and a NASTRAN solver based 3D model is used to ensure sound steady state operation at power levels up to 200 W. The QCT Phoenix is then tested at Imperial College's Plasma Propulsion Lab at anode powers between 50-115 W and mass flow rates of Xenon between 5-15 sccm. The new thruster demonstrates thrust and specific impulse of up to 2.21 mN and 274 s respectively at these low power operating conditions.

1. INTRODUCTION

The Quad Confinement Thruster (QCT) (Fig. 1) is a low power electric propulsion device that can vector thrust without requiring the use of pointing mechanisms. Invented by researchers at the Surrey Space Centre in 2010, the thruster has since undergone a number of development phases which culminated in the launch of a flight demonstration unit aboard Surrey Satellite Technology Ltd's NovaSAR-1 satellite in 2018. Despite this success, the further commercial development of the QCT has been limited by the device's poor thrust efficiency. While Hall Effect thrusters (HET) have routinely demonstrated thrust efficiencies of more than 40% [4], even at the low power levels required by small

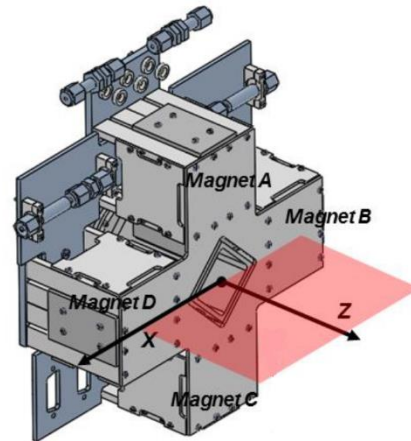satellite platforms, the QCT has not exceeded 6% [2].

Figure 1. Isometric view of the QCT CAD model with coordinate system [3]

The operating principles of the QCT are quite similar to those that govern HETs. For both thruster types, plasma is generated by the combined effects of axial electric and radial magnetic fields. The electric field is created between an anode situated at the base of the thruster's acceleration channel and a cathode positioned downstream of the channel exit (see Fig. 2). The cathode is a key component of these devices. It serves as a primary source of electrons for the ionization process and is also needed to neutralize the ion beam subsequently created.
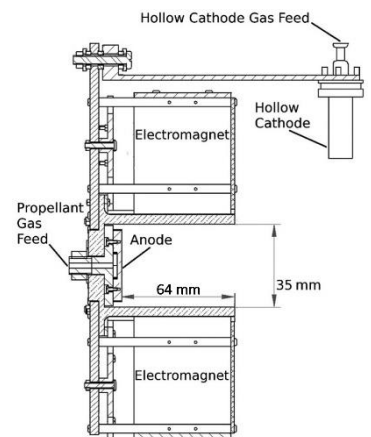

Figure 2. Cross section view of the QCT [3]

In the QCT, the magnetic field is created by eight electromagnets arranged into four pairs (see Fig. 3). The resulting magnetic field lines form four cusps along the channel walls. This characteristic magnetic topology in combination with the axial electric field creates an open rather than a closed E×B drift.
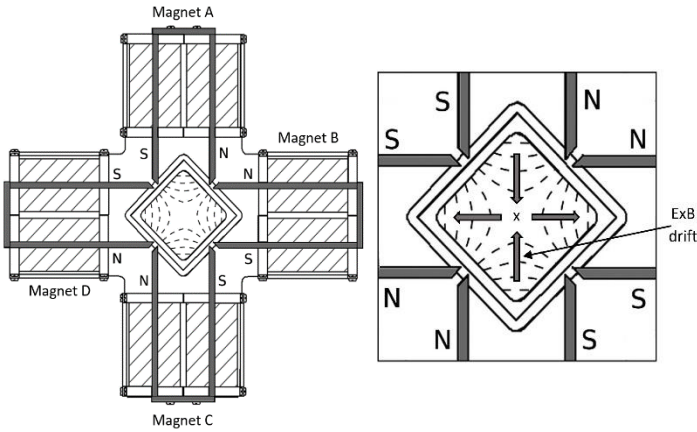
Figure 3. On the left: Top view of the QCT schematics with iron blades (grey), coils (hatched), and magnetic field lines (dashed). On the right: close up view of the magnetic field lines in the channel with ExB drift [1, 2]

As is shown in Fig. 3 the QCT's open ExB drift draws electrons along the vertical plane into the center of the channel where the magnetic flux density is lowest. We attribute the QCT's ability to function at low anode voltages (less than 100 V compared to typically more than 250 V for HETs) to the region of magnetic cancellation at the center of the channel, which provides a low impedance path between the anode and cathode of the thruster [1, 2]. Along the horizontal plane electrons are pushed into two corners of the square acceleration channel. We expect ionization to occur primarily in these zones. This was confirmed by visual observation of the plasma (see Fig. 4) during an experimental test campaign conducted at Stanford University [3].
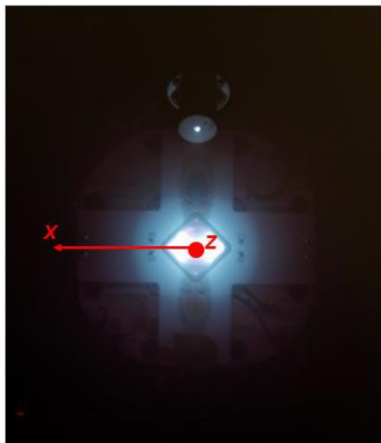

Figure 4. Bright plasma intensity regions in QCT plume [3]

The primary objectives of this test campaign were to characterize the steerability of the QCT's ion beam and to investigate the source of the device's low thrust efficiency using laser induced fluorescence (LIF). It was discovered that acceleration was taking place significantly downstream of the thruster exit plane in a semi-circular region approximately 1 cm thick, thus causing significant ion beam divergence.

As acceleration in the QCT is electrostatic, this denotes the presence of a potential drop. Similarly detached potential drops have been reported in other experimental plasma devices. They are typically defined as single or double layers [5]. During testing at different values of the magnetic field strength, it was found the position of the acceleration region remained fixed, pointing to a link between the acceleration front and QCT's electromagnetic topology.

A 3D magnetic field simulation of the QCT was built to investigate this phenomenon further. The understanding this model provided of the source of the acceleration front's characteristic shape allowed us to design a new version of the thruster, dubbed QCT Phoenix. Details on the conceptual design of this new iteration of the thruster can be found in section 3 of this paper. We then describe the processes involved in the detailed mechanical and thermal design of the novel device. Finally, sections 7 and 8 present preliminary thrust characterization results from a test campaign at Imperial College's Plasma Propulsion Lab (IPPL).

2. 3D MAGNETOSTATIC MODELLING OF THE QCT

2.1 Simulation Setup

In order to generate the 3D model of the QCT's magnetic field we used a combination of EMWork's EMS package and Matlab. First, magnetic flux density vector data generated using EMS' multicore iterative solver was saved onto an unstructured mesh. Taking care to add finer mesh controls to the inside of the thruster's channel, we set the working mesh density to 300 000+ nodes. The minimum total mesh size having been determined using the results of a convergence study. Materials used for the simulation are taken from the EMS materials library. The properties used can be found in Tab. 1 below. We used purified iron for the electromagnetic railings and cap pieces, copper for the coils, and boron nitride for the acceleration channel (all these components can be seen in Fig. 5). Once vector data had been generated by EMS, we exported the data into Matlab and interpolated it onto a Cartesian mesh grid, which enabled us to produce the 3D magnetic field lines of interest for analysis.

Table 1. Materials properties used in EMS

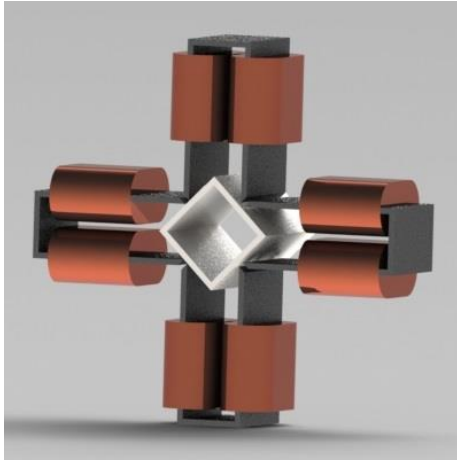|	Conductivity [Mho/m]	Relative Permeability
Air	0	1
Copper	57 000 000	0.999991
Purified Iron	11 235 000	200 000
Boron Nitride	0	1

Figure 5. Simplified SolidWorks CAD model of the QCT used in EMS [6]

2.2 Simulation Validation Against Experimental Results

Before they were used for analysis, results from the 3D model of the QCT's magnetic field were compared against results from two past experimental test campaigns.

Fig. 7 shows a 2-D map of the magnetic field strength immediately downstream of the QCT's exit plane as collected by researchers at the Surrey Space Centre using a commercial Gauss meter (Hirst GM08 handheld unit coupled with Hirst TP002 transverse Hall probe) [7]. It can clearly be seen from the figure that results from the EMS simulation match the experimental data well.
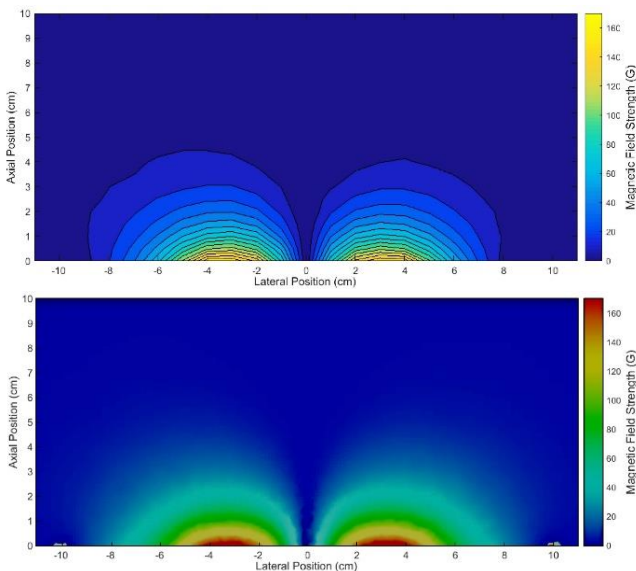

Figure 7. Magnetic field strength downstream of the thruster exit plane as measured experimentally (top) and simulated in EMS (bottom) [6]

Also used to validate the simulation were a set of axial magnetic field strength measurements taken from the top corner of the acceleration channel

using a Gauss meter. In the resulting plot (see Fig. 6) the distance scale is referenced to the thruster channel's exit plane, with negative values falling within the channel. Unlike a typical HET field profile, the magnetic field strength stays constant throughout the channel length, dropping only at the anode and channel exit. While there is a small
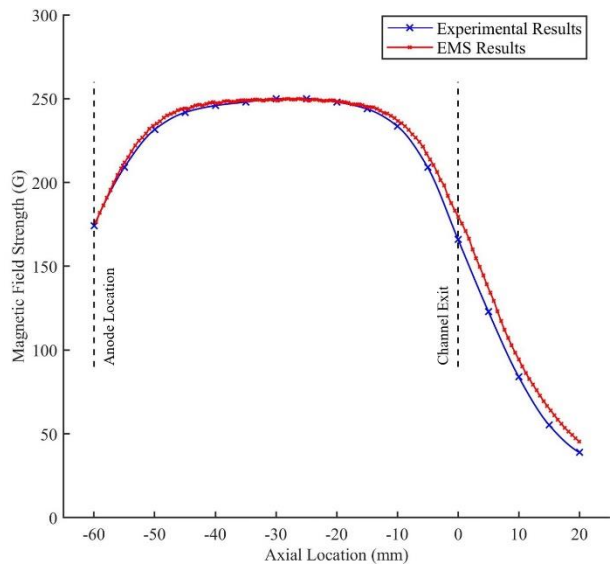

Figure 6. Axial magnetic field strength as measured experimentally and simulated in EMS [6]

mismatch between the measured and simulated magnetic field strength downstream of the channel exit, we consider that the simulation results match the global trend exhibited in the experiments satisfactorily.

2.3 QCT Simulation Results

In open channel thrusters like Hall Effect and cusped field thrusters the acceleration front is typically situated close to the exit plane [8, 9]. LIF measurements taken at Stanford revealed this was not the case for the QCT. It was found that the QCT's acceleration front was occurring 8cm downstream of the channel exit plane along a semi-circular front, in a region of low magnetic field intensity and low neutral density. Experiments further pointed to a connection between the peculiar shape and position of the acceleration front and the QCT's geometry and magnetic topology [3]. The primary objective of our 3D magnetostatic simulation was to shed light on the nature of this connection.

In the first instance, the EMS simulation was able to confirm and expand on findings from previous 2D FEMM magnetostatic simulations of the QCT. All field lines launched in between the top and bottom surfaces of the electromagnet blades within the channel (see Fig. 9) feature the QCT's signature four-point quad confinement structure in a plane perpendicular to the channel axis.
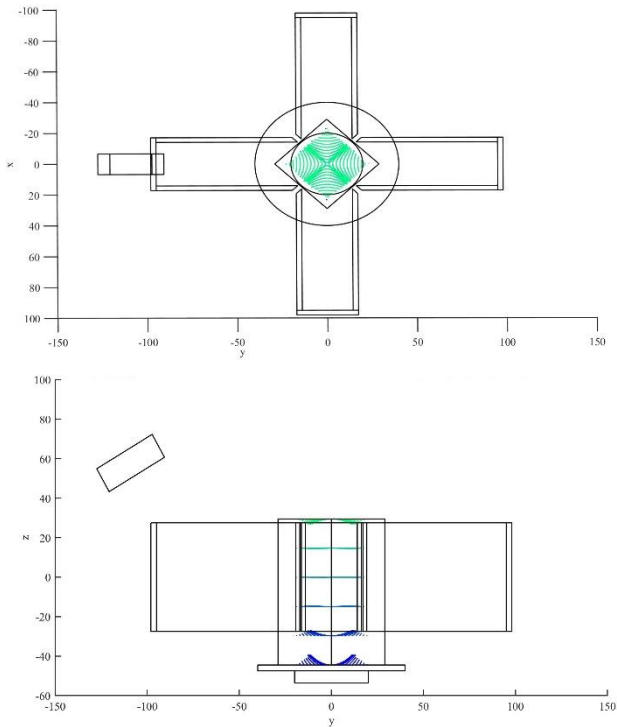
Figure 9. Top and side view of the magnetic field lines launched inside the QCT's acceleration channel [6]

The most important finding of these simulations was the 3-dimensional topology of the magnetic field lines downstream of the thruster's exit plane. Field lines launched from the cathode plane can be seen to bulge into four semi-spherical quadrants (Fig. 8). This same quad spherical structure is seen for all field lines launched downstream of the thruster exit plane. These characteristics further point to the formation of a detached single or double
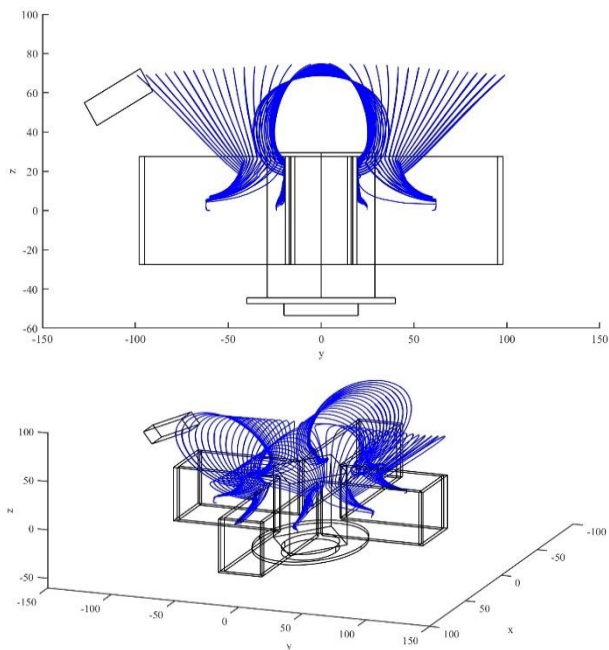

Figure 8. Side (top) and isometric (bottom) view of the QCT's magnetic field lines launched at the cathode plane [6]

layer as was posited in [3].

We speculate that electrons generated by the cathode remain attached to the field lines roughly 8 cm from the channel exit forming a thin semi-spherical zone with a high concentration of electrons. This causes a breakdown of quasi neutrality, resulting in a potential jump along the thin region. We expect ions to accelerate perpendicularly to the magnetic field lines in this region, meaning they should accelerate following the semi-spherical shape seen in Fig. 8. This expectation matches what is seen experimentally, as demonstrated by the ion velocity plots collected in [3].

The 3D characteristics of the QCT magnetic field lines downstream of the exit plane were able to provide deeper understanding for the cause of the circular shape of the acceleration front. Unfortunately, the simulation was unable to elucidate the cause for the position of the acceleration zone relative to the chamber exit plane. Having noticed that the distance between the cathode and the acceleration front is roughly equal to the height of the electromagnet blades we suggest this could be linked to the sizing of the QCT's geometry, though this would require further experiments to confirm.

3. CONCEPTUAL DESIGN OF THE QCT PHOENIX

The main focus for the re-design of the QCT was to 'flatten' the magnetic field lines downstream of the thruster channel exit plane while still maintaining the key characteristics of the QCT design as described in the introduction. The idea being that in doing so we would reduce ion beam divergence and avoid thrust efficiency loss. The secondary goal was to move the acceleration front closer to the thruster exit plane.
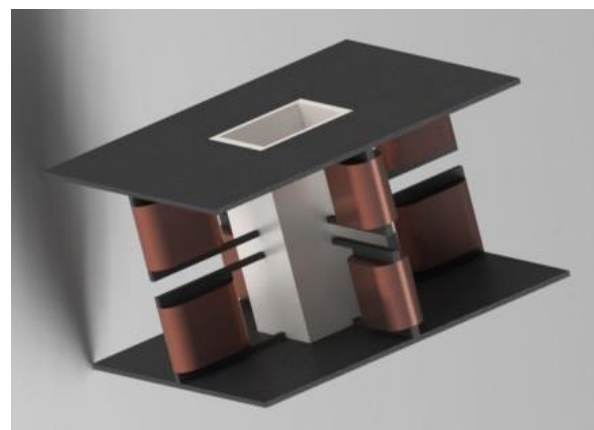

Figure 10. Isometric view of the simplified SolidWorks CAD model of the QCT Phoenix [6]

4

After multiple iterations, we arrived at the conceptual design of a new thruster, dubbed QCT Phoenix (see simplified CAD in Fig. 10). In this version of the thruster design, eight vertical electromagnets are placed on the centreline of the discharge channel walls. The electromagnets are oriented such that alternating south-south and north-north poles meet at the centre plane of the channel (Fig. 12). The channel is capped by two iron plates, intended to help capture and flatten out the magnetic field lines downstream of the exit plane.
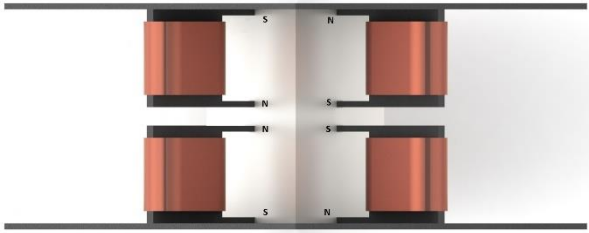

Figure 11. Side view of the simplified SolidWorks CAD model of the QCT Phoenix with magnet polarity [6]

The 3D magnetostatic field of the QCT Phoenix was simulated using the same global parameters and methodology as for the original QCT. The results of this modelling work confirmed the new design maintained key magnetic field line characteristics of the QCT. In Fig. 13 we see the QCT Phoenix features the QCT's quadrupole cusp field line pattern, meaning we still have an open E×B drift. As such, we expect that the majority of ionization would still occur primarily in two quadrants.
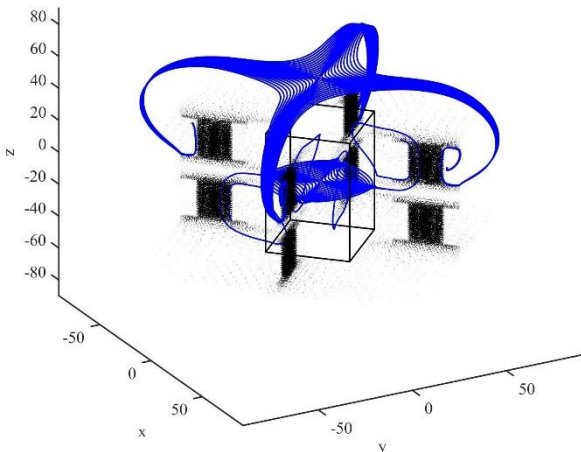

Figure 13. Isometric view of the QCT Phoenix magnetic field lines launched at the centre plane and 20 mm downstream of the exit plane [6]

Magnetic flux density characteristics were also conserved, with both thrusters presenting maximum magnetic flux density at the cusps along the walls and a null point at the channel centre (see Fig. 11). These features run the length of the acceleration channel. In preserving these characteristics, we maintain the ability to vector thrust by regulating the electromagnet current.
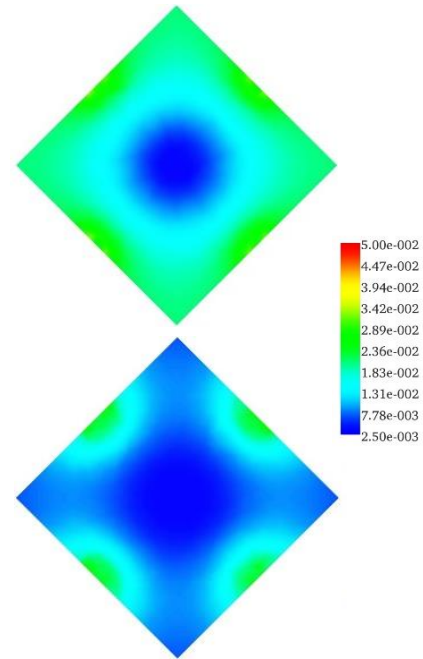

Figure 13. Top view of the magnetic flux density (in T) in the QCT (top) and QCT Phoenix (bottom) acceleration channels [6]

Fig. 14 shows that we were successful in achieving 'flat' magnetic field lines downstream of the channel exit with the new QCT Phoenix design. The 'flat' quadrupole cusp structure appears roughly 25mm downstream of the thruster exit plane for all field lines launched within the thruster channel. If our hypothesis about the link between electromagnet height and acceleration front location is correct, careful cathode positioning could place the acceleration front roughly 3cm downstream of the exit plane of the QCT Phoenix. This would be a substantial improvement over the original QCT, where the acceleration front is 8 cm downstream of the exit plane.
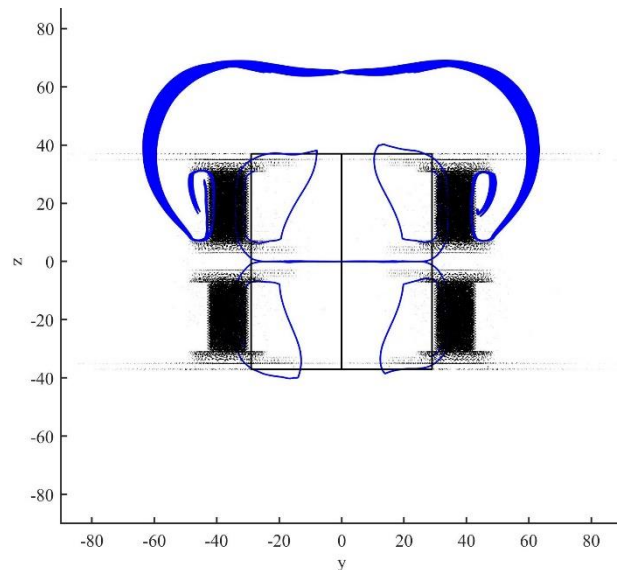

Figure 14. Side view of the QCT Phoenix magnetic field lines launched at the centre plane and 20 mm downstream of the exit plane [6]

4. MECHANICAL DESIGN OF THE QCT PHOENIX

The structural design of the QCT Phoenix was designed around the magnetic circuit which had to be contained inside a 135 x 135 x 72 mm volume. The basic layout and sizing of the electromagnet components were established in the conceptual design phase. However, some minor alterations were required to allow mounting on a support structure. Within these constraints, other parameters such as discharge channel volume, anode dimensions etc. have been chosen to match as closely as possible the original QCT to allow for an accurate comparison between the performances of the two thrusters.
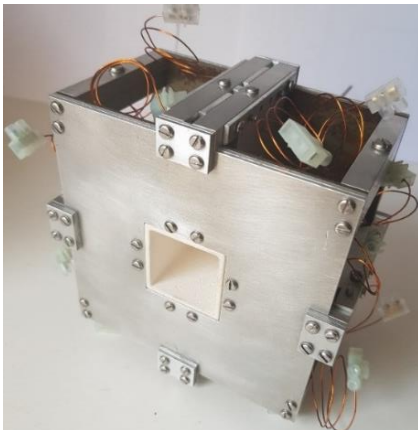

Figure 15. Isometric view of the fully assembled QCT Phoenix

4.1. Magnetic Circuit

In total, QCT Phoenix features 8 electromagnets arranged in four pairs. Their magnetic core measures 32 mm in width and 52.5 mm in height and it was constructed out of 3 layers of 1 mm electrical steel sheets that were cut in an H shape. The electromagnets were fastened on an aluminium alloy structure via 1.6 mm bolts. The coils were wound with 0.63 mm enamelled copper wire totalling at 200 turns per coil. Fig. 18 shows the shape of the electromagnets and their position inside one of the four support structures arranged around the discharge channel. These structures are mounted on a set of electrical steel and aluminium alloy plates that complete the magnetic circuit and the thruster itself. Fig. 15 shows the front and back plates and the aluminium/ electrical steel layers.
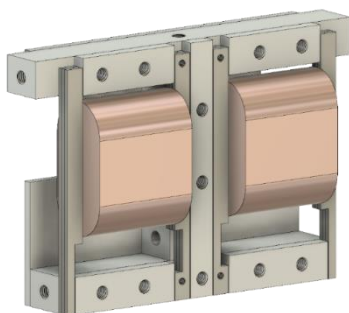

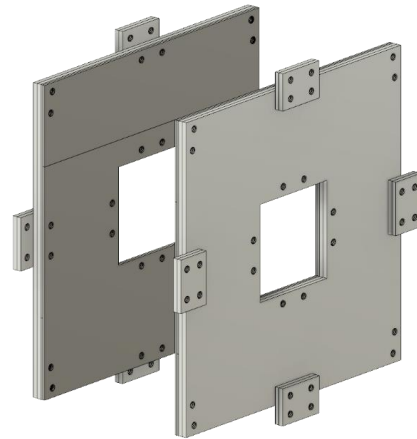*Figure 16. Electromagnet pair alignment and support structure.*

Figure 17. Aluminium support plate (light grey) and electrical steel (dark grey).

4.2. Anode, Discharge Channel and Feed Line

The discharge channel was designed to have the same volume as the QCT II version, measuring 35 mm x 35 mm length and width with 3 mm thick walls (see Fig. 17). The depth of the channel was set to 68 mm allowing for further experimentation with the anode position. For preliminary testing, the channel was cast in plaster which represents a cheap alternative to other dielectric materials such as boron nitride or alumina. The high melting point (1200 ºC) of plaster and the relatively high emissivity ε>0.75 allow for high thermal load tolerance and adequate dispersion of heat via radiation.
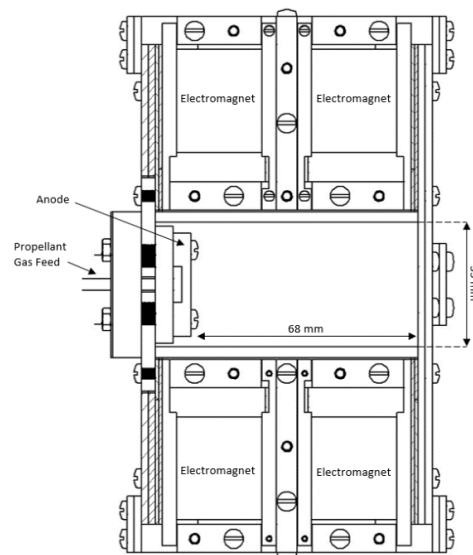

Figure 18. Cross section view of the QCT Phoenix.

The anode, which acts as a gas distributor was manufactured via CNC machining from a 5 mm thick copper plate. The high thermal conductivity of copper ensures that the heat generated from the sustained discharge is dissipated via conduction through the dielectric channel base, into the aluminium structure of the thruster.

6

A 5 mm stainless steel piece acts as a support for the anode and features a central hole where a 1/8" inch pipe was welded. It connects via a series of Swagelok connectors and a cryogenic ceramic break to the gas supply forming the feed line. Fig. 19 shows the anode-feed line assembly.
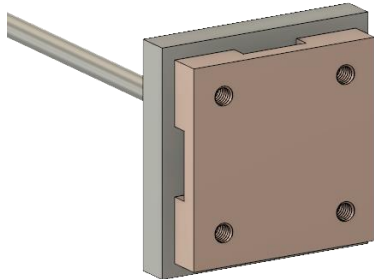

Figure 19. Anode placement on the feedline support mount

5. THERMAL SIMULATION

Given that the design process was iterative, the material choices and structural layout necessitated detailed thermal simulation to identify and avoid possible failure modes.

5.1. Software and Benchmark

Since the geometry of the QCT Phoenix is not axisymmetric, a 3D simulation had to be completed. To this end, a set of benchmark cases with the electromagnet core as the target geometry were ran at the various thermal loads and boundary conditions found in the case of thruster operation. The software used was ABAQUS, a robust, proven finite elements software, and the NASTRAN based solver used in the CAD design suit. It was found that set temperature boundaries and radiative conditions yielded identical results from the two solvers with minimal discrepancies based on slight differences in the mesh (similar node numbers and element types were enforced). However, radiative surfaces and heat source contact without a set temperature sink proved to be more difficult to solve in ABAQUS. In this case, the NASTRAN solver was more capable to accurately predict the behaviour at steady state. Furthermore, the ease of geometry export from the CAD file favoured the NASTRAN solver which was in the end chosen to simulate the thermal model of the QCT Phoenix.

5.2. Thermal Loading, Boundary Conditions, Emissivity and Failure Modes

The maximum discharge power of the QCT Phoenix was set at 200 W and a set of simulations were produced to show the thermal behaviour of the thruster under steady state operation. The electromagnet heating effects have also been simulated with a shared thermal load of 40 W corresponding to 1 A and 5 V per electromagnet.

Radiation was set as the method of heat release on the surface boundaries of the thruster under normal operation. The thrust stand itself can be regarded as a heat sink conducting heat away from the contact point with the thruster. Thus, a surface temperature condition (T=100 ºC) was set as a reasonable upper limit at the interface between the thruster and the thrust stand.

Emissivity was set at the lowest recorded values for freshly machined parts for the specific materials used. It was acknowledged that the values would change after cycled tests as the materials heat up, increasing the heat loss rates. Tab. 2 lists the values used and the critical temperature limit for the selected materials. These represent conservative values.

Table 2. Material emissivity and melting point used in the simulation.

	Emissivity, ε	Melting Point [ºC]
Al 6082	0.09	555
Copper	0.05	1085
SS 309	0.07	1480
Electrical Steel	0.07	1500
Plaster	0.75	1200

The following conditions are set as immediate failure points: 1) coil temperature above 200 ºC causing insulation failure and short circuit risk; 2) anode temperature close to the melting point (1085 ºC); 3) aluminium alloy close to the service temperature limit (200 ºC); 4) deflection over 0.5 mm causing high stress concentration at the joints.

5.3. Mesh Settings

Simplifications were made to the thruster model to reduce the computational cost of the simulation. Tetrahedral elements have been used with an adaptive base size equal to 5% of the relative diagonal of the face binding box. The total number of elements ranged from 0.8 to 2.8 million ensuring an accurate solution within 20 ºC. This was in accordance with the convergence study performed which indicated instabilities upwards from 3 million elements.

5.4. Thermal Model and Results

Temperature map and displacement results can be seen in Fig. 21 and Fig. 20 which show the QCT Phoenix operating at 200 W and being attached to the thrust stand via the top bracket which is

temperature limited to 100 ºC. In this case, coil temperatures reach 150 ºC and do not exceed the 200 ºC limit. The aluminium structure is also under the operational service temperature ensuring structural integrity. Anode temperature is well below melting, stabilizing at around 320 ºC and the deflection is below 0.15 mm therefore no stress build up is expected in the thruster upon thermal cycling. It was concluded that the thruster can sustain long term operational temperatures and can even exceed the 200 W operating point safely. Coil insulation melting is expected at 250 W discharge power.
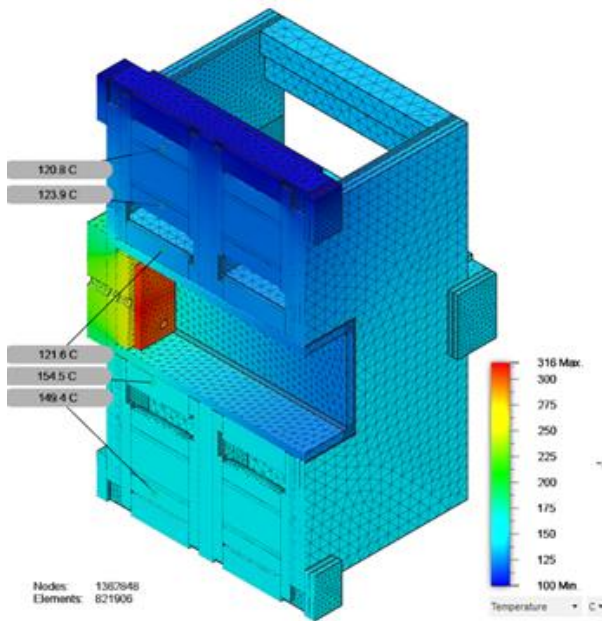

Figure 20. QCT Phoenix temperature distribution; 200 W anode discharge and 40 W summed coil
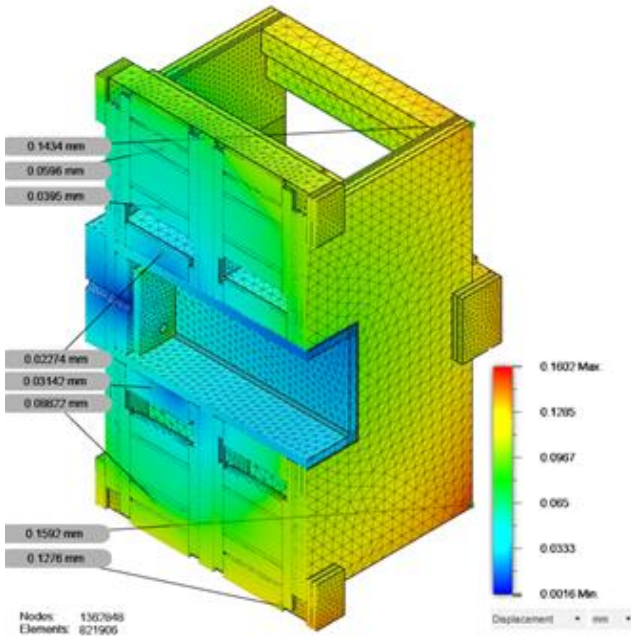

Figure 22. QCT Phoenix displacement distribution; 200 W anode discharge and 40 W summed coil power.

6. MAGNETOSTATIC SIMULATION

To finalize the design phase of the QCT Phoenix, a set of magnetostatic simulations were done to verify that the magnetic field properties closely match the values from the conceptual study. EMS was used due to the 3D effects of the quadrupole magnet pairs.

6.1. Materials, Mesh and Convergence

The materials chosen were included in the standard EMS library and correspond to electrical steel, copper and air since the simulation medium cannot be vacuum. Meshing was done with more than 300,000 nodes which ensured a converged solution in accordance with previous data from the conceptual stage. The upper bound was set at 600,000 elements. It was found that exceeding this number causes instabilities and the solution no longer converged.

6.2. Results

The magnetostatic problem was solved with a set coil currents of 1 A and the results show that the magnetic topology and field characteristics have been preserved. Fig. 22 shows the resulting field line topology to be unaffected by the structural changes.
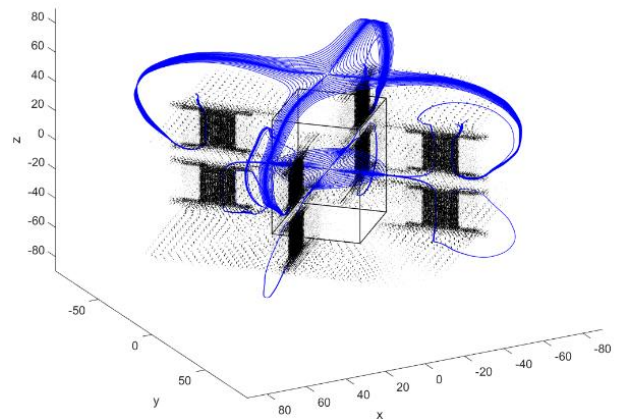

Figure 21. Magnetic field lines of the finalized design.

7. EXPERIMENTAL DESIGN

The QCT Phoenix was experimentally tested in the Boltzmann Vacuum chamber in the Imperial Plasma Propulsion Laboratory. Thrust was directly measured using a hanging pendulum type thrust balance which has been developed in collaboration with the European Space Agency (Fig. 24). Thrust measurements were taken for mass flows of 5 sccm, 10 sccm and 15 sccm of research grade xenon at discharge powers ranging from 50 W to 115 W. The beam was neutralized by a filament plasma bridge neutralizer which operated on 5 sccm of xenon for all measurements.
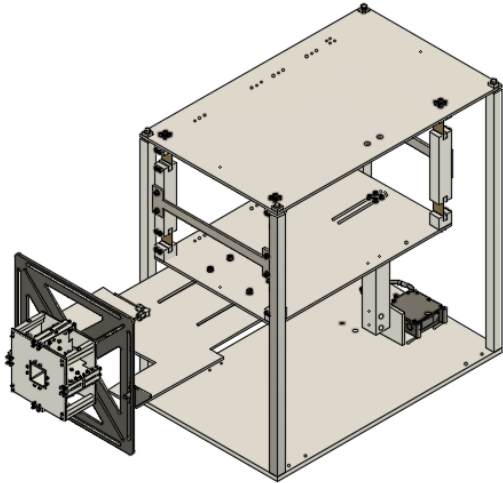
8

Figure 23. Isometric view of the QCT Phoenix mounted to the thrust balance

7.1. Vacuum Facility

The Boltzmann vacuum facility consists of a main chamber and a load lock chamber connected via a gate valve. The main chamber is 1.5 m in diameter and 2 m long, where the load lock chamber is 0.75 m in diameter and 1.5 m long. The facility utilizes a primary scroll pump, a small turbomolecular pump and two large Leybold turbomolecular pumps each with a pumping speed of 2200 L/s, along with a Leybold cryopanel at rated pumping speed of 15,000 L/s of xenon.

7.2. Thrust Balance

The hanging pendulum type thrust balance has been designed to accurately measure thrust in the range of 1 mN-1000 mN for a broad range of electric propulsion and micro-chemical propulsion systems. The balance with the thruster mounted is shown in Fig. 23.
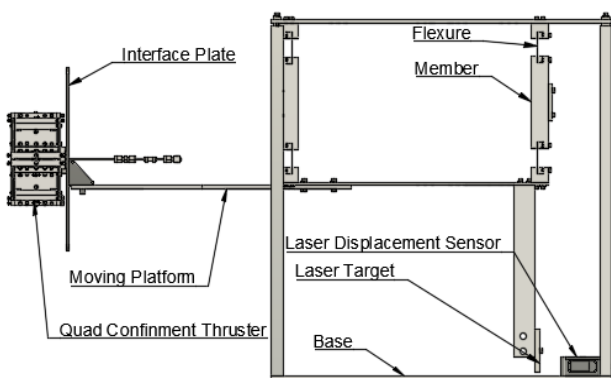

Figure 24. Labelled side view of the QCT Phoenix mounted to the thrust balance

Both the thruster and cathode (not shown in the diagram) are secured to the central platform of the

balance, such that they can float at the same electric potential. This central platform is suspended from the rest of the structure via four parallel linkages, each containing two stainless steel flexures. An optoNCDT-1750 laser triangulation sensor produced by Micro-Epsilon is used to measure the displacement of the central platform to the balance at a frequency of 2.5 Hz with sub-micron precision. The laser sensor contains an internal analog to digital converter, this allows us to communicate with the device over a digital interface, which is far less susceptible to Electromagnetic Interference (EMI) than comparable analog systems [10].

Thermal stability of the thrust balance is maintained using a closed loop self-compensating system. Before calibration or measurement the structure and central platform of the balance is heated to a predetermined set temperature using mica heaters. The temperature of the balance is monitored at several locations during operation, with the heaters being turned on an off to ensure the entire instrument stays at a fixed temperature throughout the test.

The thrust balance must be calibrated to accurately determine the relationship between the thrust produced and the displacement of the central platform of the balance. We call this relationship the sensitivity. This calibration is performed using two independent calibration systems: a Voice Coil Actuator (VCA) and a servo motor system. We begin by precisely characterizing the forces produced by the VCA over a range of currents using an independently calibrated microbalance. Before the chamber is evacuated, the VCA is positioned such that the same repeatable non-contact forces are imposed on the central platform of the balance. The displacement caused by these forces is measured using the laser sensor, such that the sensitivity can be determined. For this test, the balance showed a sensitivity of 1.462±0.071 µm/mN.

Any EMI produced by the thruster can generate currents in the VCA which will result in erroneous thrust measurements. To mitigate this, we remove the VCA prior to evacuation, and use a servo-motor to ensure the calibration does not change over time. This servo is robust to EMI, and can be commanded to pull a mass which is attached the central platform in the direction of thrust. By monitoring the displacement of the balance in response to the servo motor movement throughout the test, we can be assured the calibration has not been altered.

The balance and thruster can be seen in the setup in Fig. 27. Note that the electrical and fluidic lines have been connected from the top platform to the central platform to minimize stiffness and to ensure that any thermal expansions will not cause a force along the thrust direction.
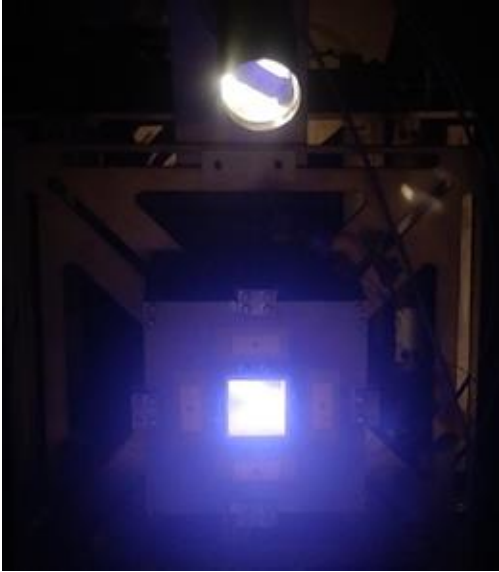
Figure 26. Front facing view of the QCT Phoenix operating.

8. RESULTS

The QCT Phoenix can be seen head on in operation in Fig. 27. Not discernible in the image, but visible through direct observation, are the bright regions appearing in two quadrants of the thruster, consistent with previous versions of the QCT.

The sensitivity of thrust of the QCT Phoenix to changes in power are shown in Fig. 25. We can see that for all three mass flows the thrust increases linearly with power, with no clear plateau. A maximum thrust of 2.21 mN is achieved at 15 sccm of xenon mass flow. Unfortunately, these thrust values are very similar to those of previous QCT type thrusters [1, 2]. Specific impulse also increases linearly with power, once again with no clear plateau. In the case of the specific impulse, the most promising values are obtained with 5 sccm of xenon flow, with a maximum of 274 s reached.
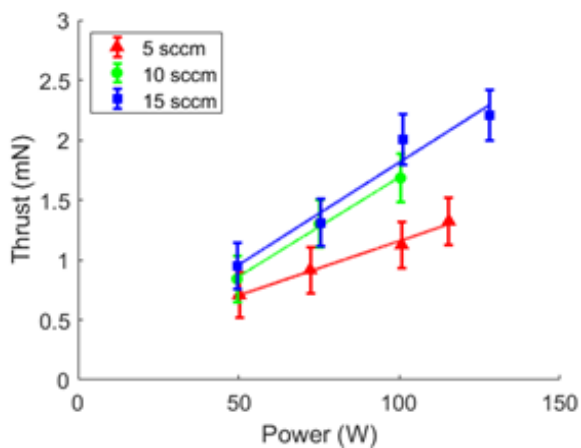

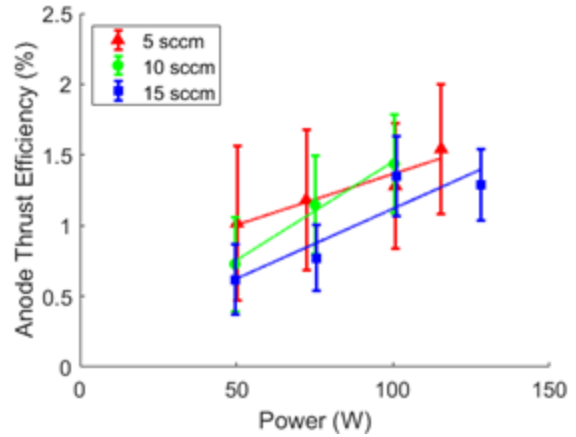*Figure 28. The sensitivity of the QCT Phoenix to anode power at different mass flows*

Figure 25. Thrust efficiency of the QCT Phoenix as a function of power
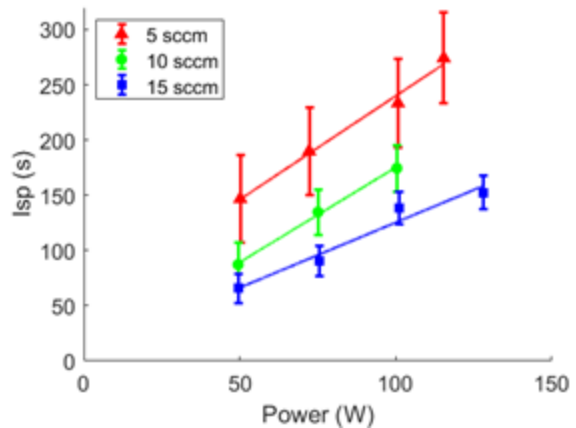

Figure 27. Specific impulse of the QCT Phoenix as a function of power

9. CONCLUSION AND NEXT STEPS

A 3D model of the QCT's magnetic field was constructed using EMS and Matlab to investigate the reason for the acceleration front's semi-circular shape. Before it was used for analysis, the model was verified against previous experimental results. It was found that the magnetostatic model matched past measurements well. The 3D model revealed the QCT's magnetic field lines bulge into four semi-spherical quadrants downstream of the thruster exit plane. This reinforces the hypothesis that electrons stay attached to the field lines downstream of the exit plane, forming a narrow semi-spherical zone causing breakdown of quasi-neutrality and as a result a potential jump. Unfortunately, the model was unable to explain the reason for the location of this region 8 cm downstream of the exit plane.

Conceptual design of a new iteration of the thruster, based on the understanding gained from this model, revolved around one primary objective: 'flattening' out the downstream field lines to reduce ion beam divergence and increase thrust efficiency. This was

successfully achieved with the QCT Phoenix and was verified using a similar methodology as in the case of the QCT. Sizing of the QCT Phoenix's electromagnets and iron caps was fixed during the conceptual design phase. All other key geometric parameters, such as the sizing of the channel cross section, were taken to match the QCT's original design.

A detailed mechanical design and thermal model of the thruster were conducted, leading to the manufacture of a thruster prototype. Magnetic components were machined out of electrical steel, and electromagnets were constructed with enamel coated copper wire. The thruster's supporting structure was machined out of aluminium. Given these material choices, and the temperature sensitive nature of electromagnets, care was taken to conduct detailed thermal simulations to ensure safe steady state operation at 200 W. Failure modes identified included coil temperature reaching more than 200 °C, the anode reaching melting temperatures, and deflection of over 0.5 mm occurring within the structure.

Preliminary performance testing of the QCT was conducted at the IPPL in the Boltzmann vacuum chamber. Thrust data was collected using the lab's newly developed hanging pendulum type balance. The thruster was operated at powers of 50 W to 115 W at mass flows ranging from 5 to 15 sccm of Xenon. A filament plasma bridge neutralizer was used for all data points collected, operating with 5 sccm of xenon. It can be easily seen from measurements that thrust, specific impulse, and anode efficiency all increase linearly with power. A maximum thrust of 2.21 mN and a maximum specific impulse of 274 s were measured. Sadly, this performance resembles what was obtained with the original QCT, meaning the updated magnetic field topology was unsuccessful in improving thruster performance. Further numerical plasma simulations will be conducted to identify the cause for this shortcoming, our objective being the creation of another iteration of the thruster design.

10. REFERENCES

1. A. Knoll, T. Harle, V. Lappas, and M. Pollard. Experimental performance characterization of a two-hundred-watt quad confinement thruster. *Journal of Propulsion and Power*, 30:1445-1449, 2014.

2. A. Knoll, D. Lamprou, V. Lappas, M. Pollard, and P. Bianco. Thrust balance characterization of a 200 W quad confinement thruster for high thrust regimes. *IEEE Transactions on Plasma Science*, 43:185-189, 2015.

3. A. L. Fabris, A. K. Knoll, C. Young, and M. Cappelli. Ion acceleration in a quad confinement thruster. In *The 35th International Electric Propulsion Conference*, 2017.

4. E. Y. Choueiri, "New Dawn for Electric Rockets," *Scientific American*, vol. 300, pp.58-65, 2009.

5. C. Charles. "A Review of Recent Laboratory Double Layers Experiments," *Plasma Sources Sci. Technol.*, 16, 2007.

6. E. Rosati Azevedo, "Magnetic Field Enhancement of the Quad Confinement Thruster," London, 2018.

7. L. Havekost, "Magnetic Field Enhancement of the Quad Confinement Thruster," Surrey, 2017.

8. A. Lucca Fabris, C.V. Young, and M.A. Cappelli. "Time-resolved laser-induced fluorescence measurement of ion and neutral dynamics in a Hall thruster during ionization oscillations," *Journal of Applied Physics*, 118(23) 233301, 2015.

9. N. MacDonald-Tenenbaum, C.V. Young, A. Lucca Fabris, M. Nakles, W. Hargus Jr., M.A. Cappelli. "Time-Synchronized Continuous Wave Laser Induced Fluorescence Velocity Measurements of a 600 Watt Hall Thruster," In *The 34th International Electric Propulsion Conference*, 2015.

10. S. Pottinger, D. Lamprou, A. Knoll, and V. Lappas, "Impact of plasma noise on a direct thrust measurement system," *Review of Scientific Instruments* 83, 033504 (2012)